

Analysis of oscillations of atmospheric neutrinos

G.L. Fogli^a, E. Lisi^{a*}, A. Marrone^a, and D. Montanino^b

^aDipartimento di Fisica and Sezione INFN di Bari, Via Amendola 173, 70126 Bari, Italy

^bDipartimento di Scienza dei Materiali dell'Università di Lecce, Via Arnesano, 73100 Lecce, Italy

We briefly review the current status of standard oscillations of atmospheric neutrinos in schemes with two, three, and four flavor mixing. It is shown that, although the pure $\nu_\mu \rightarrow \nu_\tau$ channel provides an excellent 2ν fit to the data, one cannot exclude, at present, the occurrence of additional subleading $\nu_\mu \rightarrow \nu_e$ oscillations (3ν schemes) or of sizable $\nu_\mu \rightarrow \nu_s$ oscillations (4ν schemes). It is also shown that the wide dynamical range of energy and pathlength probed by the Super-Kamiokande experiment puts severe constraints on nonstandard explanations of the atmospheric neutrino data, with a few notable exceptions.

1. Introduction

It is well known that the Super-Kamiokande (SK) atmospheric neutrino data can be beautifully explained in terms of 2ν oscillations in the $\nu_\mu \rightarrow \nu_\tau$ channel [1]. This interpretation is also supported by MACRO [2] and by Soudan2 [3]. Conversely, pure $\nu_\mu \rightarrow \nu_e$ oscillations do not provide a good fit to the SK data [4], and are independently excluded by the negative ν_e disappearance searches in the CHOOZ [5] and Palo Verde [6] reactors. Pure $\nu_\mu \rightarrow \nu_s$ oscillations (ν_s being a hypothetical sterile neutrino) are also disfavored by SK [1,7] (and by MACRO [2]), due to nonobservation of the associated matter effects [8] and neutral current event depletion [9].

Although two-flavor $\nu_\mu \rightarrow \nu_\tau$ oscillations represent the most economical explanation, it should be stressed that, to some extent, additional oscillation channels may be open, as naturally expected in 3ν and 4ν schemes [10] accommodating the current phenomenology. Moreover, ν_μ disappearance might be driven by dynamics different from the simple mass-mixing mechanism. In this article, we briefly review the status of such solutions, with emphasis on: (i) scenarios involving more than two states (3ν and 4ν mixing), and (ii) scenarios involving nonstandard dynamics (decay, extra dimensions, decoherence).

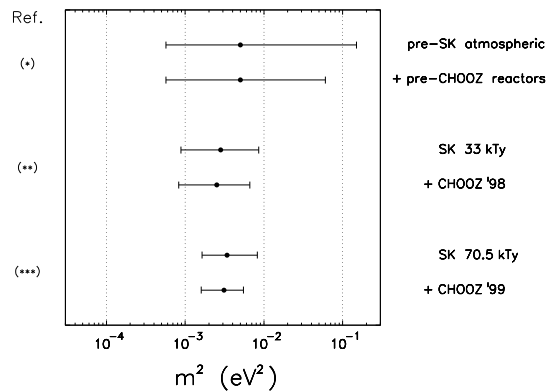
2. 3ν oscillations

Assuming that two out of three active ν 's are almost degenerate (say, $m_1 \simeq m_2$), it can be shown [4] that atmospheric ν 's probe only $m^2 \equiv m_3^2 - m_{1,2}^2$ and the mixing matrix elements $U_{\alpha 3}$:

$$3\nu \text{ parameter space} \equiv (m^2, U_{e3}^2, U_{\mu 3}^2, U_{\tau 3}^2), \quad (1)$$

with $U_{e3}^2 + U_{\mu 3}^2 + U_{\tau 3}^2 = 1$ for unitarity.

Progress in m^2 bounds for unconstrained 3ν mixing
(90% C.L., $N_{\nu} = 3$)



(*) G.L. Fogli, E. Lisi, D. Montanino, and G. Scioscia, Phys. Rev. D 55, 4385 (1997)
 (**) G.L. Fogli, E. Lisi, A. Marrone, and G. Scioscia, Phys. Rev. D 59, 033001 (1999)
 (***) G.L. Fogli, E. Lisi, A. Marrone, and D. Montanino Proceedings of Neutrino2000

Figure 1. Progress in bounds on m^2 , as derived by 3ν analyses of atmospheric and reactor data, both before and after SK and CHOOZ.

*Speaker. E-mail: lisi@ba.infn.it

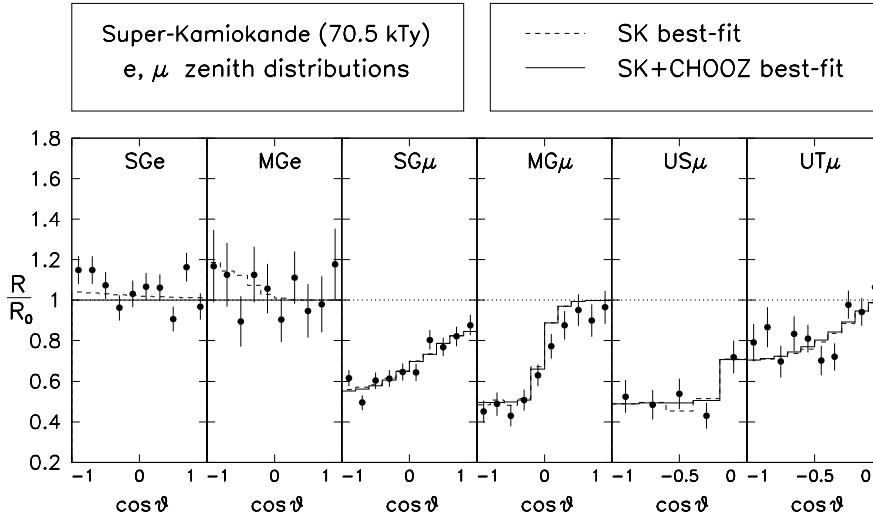


Figure 2. SK zenith distributions, normalized to no-oscillation expectations. Dots with error bars: SK data. Dashed and solid lines: best fits to SK only and to SK+CHOOZ [11].

We present a preliminary update [11] of previous limits [4] on such parameters, using the latest data from SK (70.5 kTy) [1] and CHOOZ [5]. The SK data include 55 zenith bins: 10+10 bins for the subGeV (SG) $e+\mu$ events, 10+10 bins for the multiGeV (MG) $e+\mu$ events, and 5+10 bins for the upward stopping (US) and through-going (UT) μ events. For CHOOZ, we use the total rate (one datum). We accurately calculate all such observables, and χ^2 -fit them (see [4] for details).

Figure 1 shows that the allowed range for m^2 is stable around $3 \times 10^{-3} \text{ eV}^2$. The same figure also shows the impact of SK and CHOOZ in sharpening [11,4] prior bounds on m^2 [12].

Figure 2 shows the SK data and the best-fit theoretical distributions. The best fit for SK data only ($\chi^2 = 47.5$, dashed line) is found at

$$(m^2, U_{e3}^2, U_{\mu3}^2, U_{\tau3}^2) \simeq (3.5, 0.07, 0.57, 0.36), \quad (2)$$

where $[m^2] = 10^{-3} \text{ eV}^2$. For $U_{e3}^2 = 0.07$, the theoretical MGe distribution shows a distortion which, however, is well within the uncertainties. The weak preference for $U_{e3}^2 \neq 0$ is suppressed by CHOOZ data. The SK+CHOOZ best fit ($\chi^2 = 49$, solid lines) basically corresponds to pure $\nu_\mu \rightarrow \nu_\tau$ oscillations with maximal mixing,

$$(m^2, U_{e3}^2, U_{\mu3}^2, U_{\tau3}^2) \simeq (3.0, 0, 0.5, 0.5), \quad (3)$$

with limited allowance for extra ν_e mixing [11],

$$\text{SK data only} : U_{e3}^2 < 0.31 \quad (0.38), \quad (4)$$

$$\text{SK + CHOOZ} : U_{e3}^2 < 0.04 \quad (0.07), \quad (5)$$

the bounds being at 90 (99%) C.L. for 3 d.o.f. Unfortunately, it appears very difficult to probe (through present atmospheric data) values of U_{e3}^2 as small as a few %, which may entail interesting Earth matter effects [4,13]. Constraining U_{e3}^2 is a major task for future atmospheric [14], reactor [15] and accelerator [16] ν experiments.

The bounds on 3ν mixing are more evident in the $(\nu_e, \nu_\mu, \nu_\tau)$ triangle plot, embedding the unitarity constraint (see [4,12] for details). Figure 3 shows the allowed regions in such triangle, whose lower and right sides represent the subcases of pure $\nu_\mu \rightarrow \nu_\tau$ (allowed) and pure $\nu_\mu \rightarrow \nu_e$ (excluded). Large ν_e mixing is allowed by SK alone, but not by the SK+CHOOZ combination, where only a narrow region survives near the lower side of the triangle. In such region, $U_{\mu3}^2 \sim U_{\tau3}^2$ within a factor of two [e.g., $(U_{\mu3}^2, U_{\tau3}^2) \simeq (2/3, 1/3)$ is also allowed]. In conclusion, the 3ν analysis of SK+CHOOZ shows that the $\nu_\mu \rightarrow \nu_e$ channel might be open with a few % amplitude. Future atmospheric, reactor, and accelerator ν experiments will test this interesting possibility.

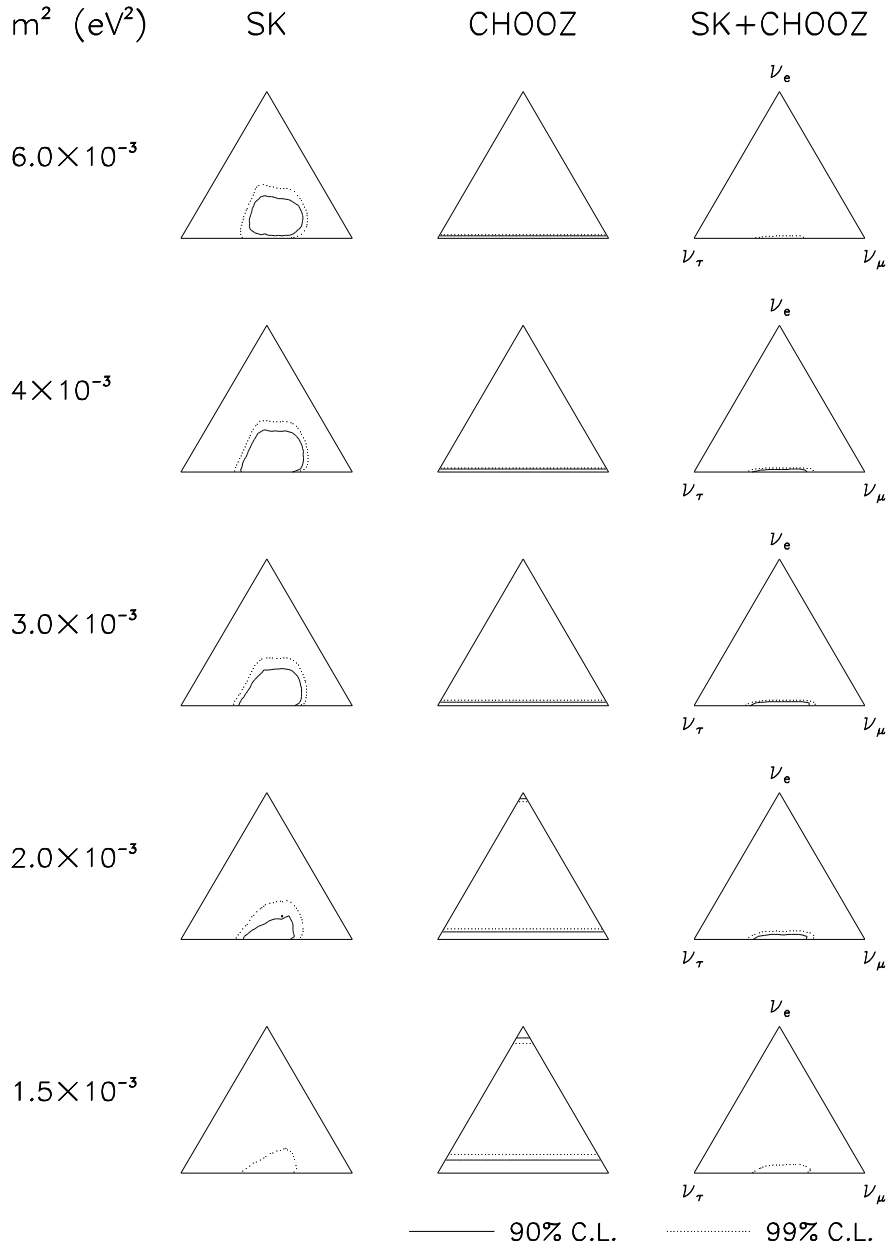


Figure 3. Three-flavor analysis in the $(\nu_e, \nu_\mu, \nu_\tau)$ triangle plot, for five representative values of m^2 . Left and middle column: separate analyses of Super-Kamiokande 70.5 kTy data and CHOOZ final data, respectively. Right column: combined SK+CHOOZ allowed regions. The SK+CHOOZ solutions are close to pure $\nu_\mu \leftrightarrow \nu_\tau$ oscillations, with upper limits on U_{e3}^2 in the few percent range [11].

3. 4ν oscillations

The current evidence for ν oscillations coming from solar, atmospheric, and LSND data can be accommodated by introducing a fourth, sterile neutrino state ν_s [10]. The mass spectrum seems then to be favored in the “2+2” form (two separated doublets) [17], although the “3+1” option (triplet plus singlet) is not dismissed [18].

In 2+2 models, it is often assumed that atmospheric ν oscillations involve *either* the $\nu_\mu \rightarrow \nu_\tau$ or the $\nu_\mu \rightarrow \nu_s$ channel. Correspondingly, it is assumed that solar ν oscillations involve *either* the $\nu_e \rightarrow \nu_s$ or the $\nu_e \rightarrow \nu_\tau$ channel. Such simplifying assumptions are challenged by the most recent SK data [1,19], which disfavor oscillations into ν_s for both atmospheric and solar neutrinos. However, it should be realized that atmospheric ν_μ 's and solar ν_e 's may also oscillate into *linear combinations* of ν_s and ν_τ [20] (rather than into ν_s and ν_τ separately), e.g.,

$$\text{atm. neutrino oscillations} : \nu_\mu \rightarrow \nu_+ , \quad (6)$$

$$\text{solar neutrino oscillations} : \nu_e \rightarrow \nu_- , \quad (7)$$

where

$$\begin{pmatrix} \nu_+ \\ \nu_- \end{pmatrix} = \begin{pmatrix} +\cos\xi & +\sin\xi \\ -\sin\xi & +\cos\xi \end{pmatrix} \begin{pmatrix} \nu_\tau \\ \nu_s \end{pmatrix} , \quad (8)$$

with ξ to be constrained by experiments. A recent analysis of $\nu_e \rightarrow \nu_-$ solar oscillations shows that all the usual solutions (MSW or vacuum) are compatible with solar data for $\sin^2\xi > 0.3$ [21].

Concerning atmospheric ν 's, we have analyzed [22] the same data as in Fig. 2 for $\xi \in [0, \pi/2]$. Figure 4 shows some representative results of the χ^2 fit, as a function of the mass square difference m^2 . The fit for unconstrained ξ (thick solid line) is almost equal to the one for $\xi = 0$ (pure $\nu_\mu \rightarrow \nu_\tau$, thin solid line), implying that the SK data prefer small or zero admixture of ν_s . The case $\xi = \pi/2$ (pure $\nu_\mu \rightarrow \nu_s$, dashed line) leads to $\Delta\chi^2 \simeq 15$ and is disfavored. However, the case $\xi = \pi/4$ (fifty-fifty admixture of ν_τ and ν_s , dotted line) leads only to a modest increase in χ^2 and cannot be excluded.

The 4ν analysis can also be done in a triangle plot (different from the 3ν case) embedding the $(\nu_\mu, \nu_s, \nu_\tau)$ unitarity constraint [22]. Figure 5

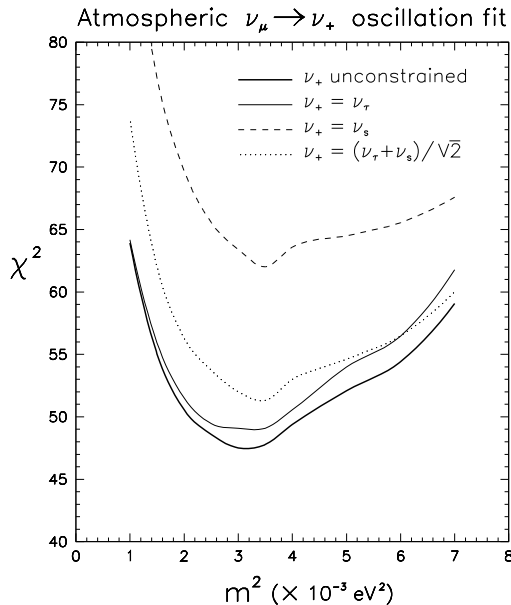


Figure 4. χ^2 fit of 55 SK data bins (70.5 kTy) for $\nu_\mu \rightarrow \nu_+$ oscillations, under various assumptions for the ν_s component of ν_+ . A large ν_s component (e.g., 50%, dotted line) is not excluded [22].

shows the results for separate and combined SK data sets. It can be seen that, in the combination, the case of pure $\nu_\mu \rightarrow \nu_\tau$ oscillations (left side) is allowed, while the case of pure $\nu_\mu \rightarrow \nu_s$ oscillations (right side) is significantly disfavored. However, there are intermediate solutions for $\sin^2\xi < 0.7$ which have a significant admixture of ν_s . Such results and constraints emerge from the interplay of low-energy data (which are more sensitive to m^2) and high-energy data (more sensitive to the ν_s component through matter effects, scaling as $\frac{1}{2}$ neutron density $\times \sin^2\xi$ [22]).

A qualitative comparison between such results [22] and those in [21] indicates that atmospheric ν data can be reconciled with any of the oscillation solutions to the solar ν problem in the range $0.3 < \sin^2\xi < 0.7$. A somewhat different 4ν analysis [23] derives similar conclusions. Summarizing, it turns out that world ν oscillation data are consistent with 4ν solutions to the solar and atmospheric anomalies, involving oscillations into both active and sterile states at the same time.

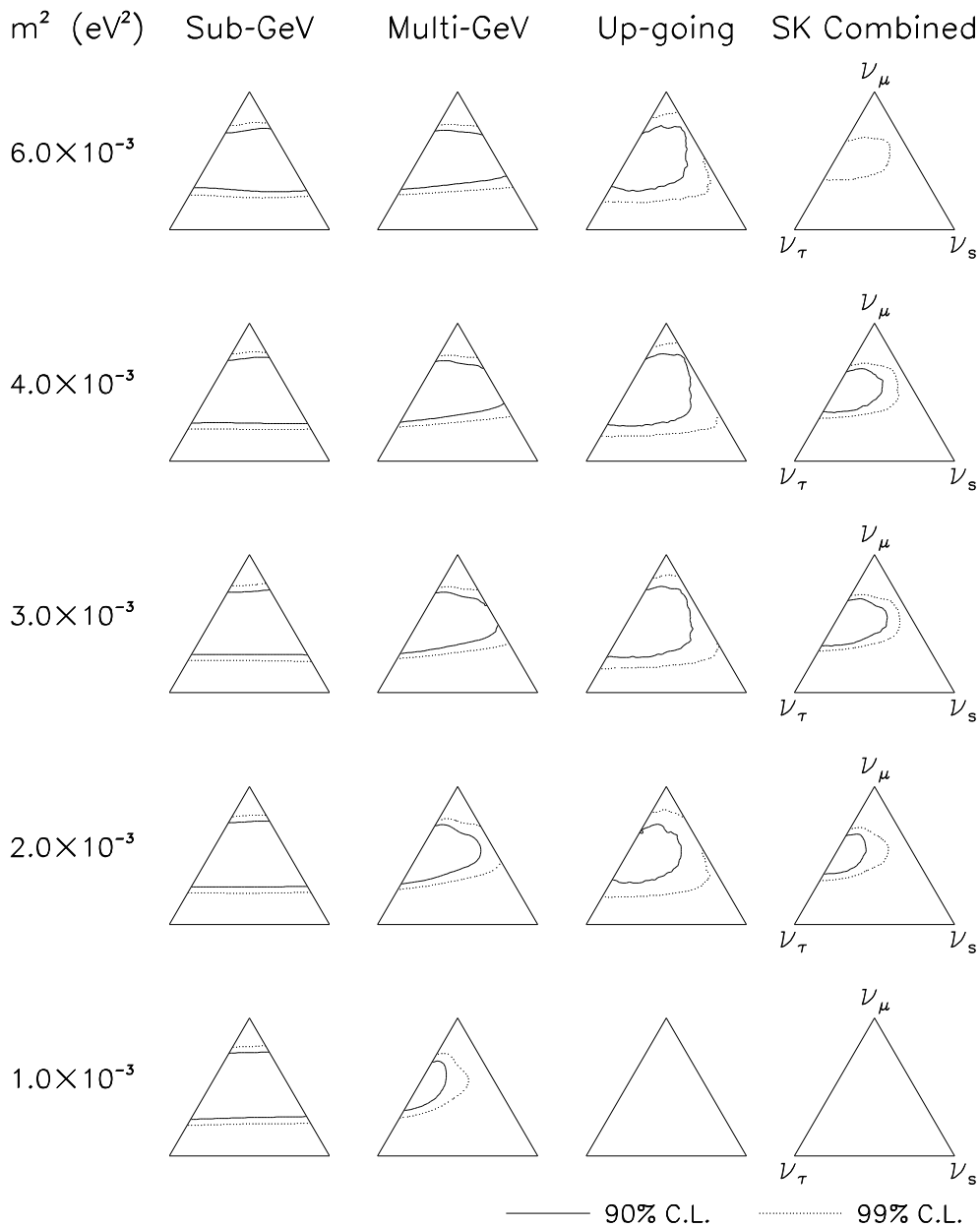


Figure 5. 4ν analysis in the $(\nu_\mu, \nu_s, \nu_\tau)$ triangle plot, for five representative values of m^2 . First three columns: separate analyses of SGe+SG μ , MGe+MG μ , and US μ +UT μ data. Right column: all SK data (70.5 kTy). The allowed regions typically include pure $\nu_\mu \leftrightarrow \nu_\tau$ oscillations (left side of the triangle) and disfavor pure $\nu_\mu \rightarrow \nu_s$ oscillations (right side of the triangle). However, intermediate situations with ν_μ mixing with both ν_τ and ν_s are allowed inside the triangle [22].

4. Nonstandard dynamics

The SK data probe three decades in pathlength L and four decades in energy E . Such a wide dynamical range severely constrains deviations from the standard L/E behavior of the $P_{\mu\tau}$ transition probability, which are expected in the presence of exotic dynamics [24] (e.g., violations of relativity principles [25,26], which lead to a $L \cdot E$ behavior).

An analysis of older data (45 kTy) has shown that, assuming a $L \cdot E^n$ dependence of the phase, the SK measurements constrain n to be very close to -1 , thus favoring standard oscillations, and excluding several nonstandard explanations [27]. Such results, shown in Fig. 6, have been strengthened by the latest SK data [1]. A peculiar FCNC scenario with $n = 0$ [28] is also strongly disfavored—as any energy independent mechanism for ν_μ disappearance—by combining low and high energy SK data [29]. Therefore, $P_{\mu\tau}$ seems to be (dominantly) a function of L/E .

However, is $P_{\mu\tau}$ necessarily a *periodic* function of L/E ? The answer is, surprisingly, no. There are (at least) three exotic scenarios which predict a *monotonic* decrease of the oscillation probability in the relevant L/E range, and that are anyway reasonably consistent with the data.

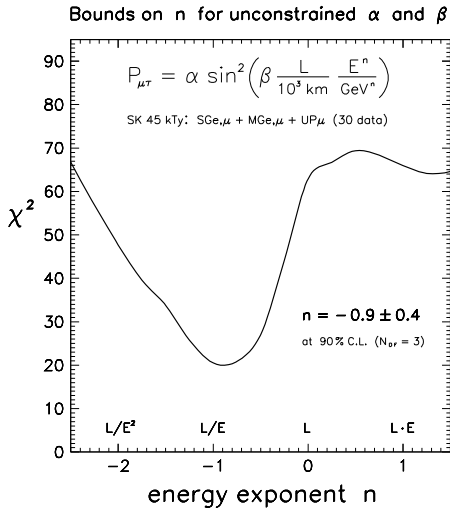


Figure 6. Bounds on the energy exponent n , assuming oscillation phase $\propto L \cdot E^n$. (Older 45 kTy SK data used in this figure [27].)

The first scenario involves ν decay [30], with a decay length of the order of the Earth radius. The second scenario [31] assumes ν_μ mixing with neutrino states propagating in large extra dimensions [32]. A third scenario [33] assumes nonstandard Liouville dynamics [34], leading to ν decoherence and thus to a damping of oscillations. Figure 7 shows that the best fit for pure decoherence does not differ significantly from the standard oscillation one [33]. The two cases shown in Fig. 7 correspond to different functional forms for $P_{\mu\mu}$,

$$\text{oscillation : } P_{\mu\mu} \simeq \frac{1}{2}[1 + \cos(+\rho L/E)] , \quad (9)$$

$$\text{decohere. : } P_{\mu\mu} \simeq \frac{1}{2}[1 + \exp(-\rho L/E)] , \quad (10)$$

with $[E] = \text{GeV}$, $[L] = \text{km}$, and $\rho \simeq 7 \times 10^{-3} \text{ GeV/km}$ in both cases. Such forms have the same asymptotic behavior, namely, $\langle P_{\mu\mu} \rangle \simeq 1(\frac{1}{2})$ for small (large) L/E , but they significantly differ for intermediate values of L/E where, however, the large energy-angle smearing of SK prevents a clear discrimination.

Although such nonstandard explanations [30, 31,33] of SK data do not survive Occam's razor, they survive the current experimental tests for a simple reason: the oscillation pattern (appearance of ν_τ and re-appearance of ν_μ) has not been directly observed so far, and a monotonic ν_μ disappearance is not excluded yet. Therefore, the unambiguous observation of an oscillation cycle represents an important task for future atmospheric [14] and accelerator [16] ν experiments.

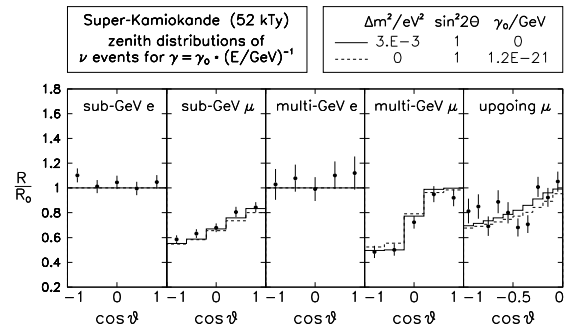


Figure 7. Comparison of standard oscillations (solid line) vs neutrino decoherence (dashed line) as explanation of the SK data. See [33] for details.

5. Conclusions

Two-flavor $\nu_\mu \rightarrow \nu_\tau$ oscillations represent a simple and beautiful explanation of the SK data (as well as of MACRO and Soudan2). However one cannot exclude, in addition, subleading $\nu_\mu \rightarrow \nu_e$ transitions (possible in 3ν models) or sizable $\nu_\mu \rightarrow \nu_s$ transitions (possible in 4ν models). Moreover, the nonobservation of an oscillation cycle still leaves room for exotic dynamics. Further experimental and theoretical work is needed to firmly establish both the flavors and the dynamics involved in atmospheric ν_μ disappearance.

REFERENCES

1. H. Sobel, these Proceedings.
2. B. Barish, these Proceedings.
3. T. Mann, these Proceedings.
4. G.L. Fogli, E. Lisi, A. Marrone, and G. Scioscia, Phys. Rev. D **59**, 033001 (1999).
5. CHOOZ coll., Phys. Lett. B **466**, 415 (1999).
6. G. Gratta, these Proceedings.
7. SK collaboration, hep-ex/0009001.
8. E. Akhmedov, P. Lipari, and M. Lusignoli, Phys. Lett. B **300**, 128 (1993); P. Lipari and M. Lusignoli, Phys. Rev. D **58**, 073005 (1998); Q.Y. Liu and A.Yu. Smirnov, Nucl. Phys. B **524**, 505 (1998); Q.Y. Liu, S.P. Mikheyev, and A.Yu. Smirnov, Phys. Lett. B **440**, 319 (1998); N. Fornengo, M.C. Gonzalez-Garcia, and J.W.F. Valle, Nucl. Phys. B **580**, 58 (2000).
9. F. Vissani and A.Yu. Smirnov, Phys. Lett. B **432**, 376 (1998); L.J. Hall and H. Murayama, Phys. Lett. B **436**, 323 (1998).
10. See talks by B. Kayser, R. Mohapatra, and A.Yu. Smirnov, these Proceedings.
11. G.L. Fogli, E. Lisi, and A. Marrone, work in progress.
12. G.L. Fogli, E. Lisi, D. Montanino, and G. Scioscia, Phys. Rev. D **55**, 4385 (1997).
13. S.T. Petcov, Phys. Lett. B **434**, 321 (1998); E. K. Akhmedov, A. Dighe, P. Lipari, and A.Yu. Smirnov, Nucl. Phys. B **542**, 3 (1999); J. Pantaleone, Phys. Rev. Lett. **81**, 5060 (1998); G.L. Fogli, E. Lisi, A. Marrone, and D. Montanino, Phys. Lett. B **425**, 341 (1998); A. De Rujula, M.B. Gavela, and P. Hernandez, hep-ph/0001124.
14. A. Geiser, these Proceedings.
15. L. Mikaelyan, these Proceedings.
16. See talks by A. De Rujula, K. Nakamura, A. Rubbia, and S. Wojcicki, these Proceedings.
17. S.M. Bilenky, C. Giunti, and W. Grimus, in *Neutrino '96* (World Scientific, 1997), p.174; V. Barger, S. Pakvasa, T.J. Weiler, and K. Whisnant, Phys. Rev. D **58**, 093016 (1998).
18. V. Barger, B. Kayser, J. Learned, T. Weiler, and K. Whisnant, hep-ph/0008019.
19. Y. Suzuki, these Proceedings.
20. See, e.g., D. Dooling, C. Giunti, K. Kang, and C.W. Kim, Phys. Rev. D **61**, 073011.
21. C. Giunti, M.C. Gonzalez-Garcia, and C. Peña-Garay, Phys. Rev. D **62**, 013005 (2000); M.C. Gonzalez-Garcia, these Proceedings.
22. G.L. Fogli, E. Lisi, and A. Marrone, "Four neutrino oscillation solutions of the atmospheric neutrino anomaly", to appear.
23. O. Yasuda, hep-ph/0006319.
24. P. Lipari and M. Lusignoli, Phys. Rev. D **60**, 013003 (1999); G.L. Fogli, E. Lisi, A. Marrone, and G. Scioscia, Phys. Rev. D **59**, 117303 (1999).
25. M. Gasperini, Phys. Rev. D **38**, 2635 (1988).
26. S. Coleman and S.L. Glashow, Phys. Lett. B **405**, 249 (1997); S.L. Glashow, A. Halprin, P.I. Krastev, C.N. Leung, and J. Pantaleone, Phys. Rev. D **56**, 2433, 1997.
27. G.L. Fogli, E. Lisi, A. Marrone, and G. Scioscia, Phys. Rev. D **60**, 053006 (1999).
28. M.C. Gonzalez-Garcia *et al.*, Phys. Rev. Lett. **82**, 3202 (1999).
29. M.M. Guzzo, H. Nunokawa, O.L.G. Peres, and R. Zukanovich Funchal, Nucl. Phys. B (Proc. Suppl.) **87**, 201 (2000).
30. V. Barger, J.G. Learned, P. Lipari, M. Lusignoli, S. Pakvasa, and T.J. Weiler, Phys. Lett. B **462**, 109 (1999).
31. R. Barbieri, P. Creminelli, and A. Strumia, hep-ph/0002199.
32. K. Dienes, these Proceedings.
33. E. Lisi, A. Marrone, and D. Montanino, Phys. Rev. Lett. **85**, 1166 (2000).
34. F. Benatti and R. Floreanini, JHEP **2**, 32 (2000).